Carbohydrate Polymers 88 (2012) 1445–1452

Contents lists available at SciVerse ScienceDirect

Carbohydrate Polymers

journal homepage: www.elsevier.com/locate/carbpol

Synthesis and characterization of a degradable composite agarose/HA hydrogel

Ling-Min Zhang, Chao-Xi Wu, Jian-Yan Huang, Xiao-Hui Peng, Peng Chen, Shun-Qing Tang*

Biomedical Engineering Institute, Jinan University, Guangzhou 510632, China

ARTICLE INFO

Article history:
Received 22 November 2011
Received in revised form 7 February 2012
Accepted 19 February 2012
Available online 25 February 2012

Keywords:
Agarose
Hyaluronic acid
Hydrogel
Biodegradation

ABSTRACT

Biodegradable hydrogels are useful for tissue engineering. In this study, we developed a new type of biodegradable composite agarose/HA hydrogel derived from agarose and hyaluronic acid, with epichlorohydrin (ECH) as crosslinking agent. The crosslinking structures, thermal stability and pore morphologies of the composite agarose/HA hydrogel were characterized by Fourier transformed infrared (FTIR) spectroscopy, scanning electronic microscopy (SEM) and thermal gravimetric analysis (TGA). The composite agarose/HA hydrogel showed no any cytotoxic effect to 3T3 fibroblast by MTT test and its degradation time in vivo can be controlled by altering the component ratios of agarose and HA, with degradation time ranging from 4 wk to 8 wk. These findings demonstrate that the composite hydrogel has a potential in tissue engineering applications, wound healing and drug delivery.

1. Introduction

Hydrogel is uniquely and widely applied because of the easily tailored properties and convenient operation in clinical (Hawkins, Milbrandt, Puleo, & Hilt, 2011). Some advantages are as follows, hydrogel can be implanted in human body with small surgical wound, and bioactive molecules or cells for therapy can be directly incorporated into hydrogel. The gel formation in situ by chemically crosslinking or physical gelation has recently been paid much attention. But the disadvantages are also evident, for example the residual monomers or crosslinking agents used for chemically crosslinked hydrogel are usually toxic or the reaction process emits large amount of heat, and the physical gels through phase transition have difficulty in ensuring the integration of different components. For another option, a crosslinking hydrogel prepared in vitro can still be considered as a useful candidate for biomedical applications.

Biodegradation is considered as a critical requirement for most hydrogel biomedical applications since it is difficult to surgically remove hydrogel from body in most cases (Deshmukh et al., 2010). However, controlling the degradation rate of hydrogel is still a challenge to its applications in tissue engineering and wound dressing for extensive wound at present. Hyaluronic acid (HA) is a degradable, nonsulfated glycosaminoglycan and a major component of extracellular matrix (ECM) for nearly all mammalian connective tissues with multiple biological functions (Toole, 2004). HA accumulated during morphogenesis, may contribute to fetal scarless healing, and plays a role in wound healing. Of relevance to bone, HA has been found in high concentration in the early fracture callus, and in lacunae surrounding hypertrophic chondrocytes in the growth plate and in the cytoplasm of osteoprogenitor cells. However, the poor mechanical properties, rapid degradation and clearance in vivo without crosslinking limit clinical applications of HA (Segura et al., 2005). Scaffolds for regenerative medicine application should be degraded over the course of tissue regeneration to allow complete repair by host tissue. For retarding degradation of HA, chemical crosslinking or compositing HA with other slow or no degradation polymer is advisable choice. It is of great interest to cross-link HA into hydrogel for improving mechanical properties and controlling residence time (i.e., controlled degradation, metabolism, and clearance) (Choh, Cross, & Wang, 2011).

Agarose is a typical polysaccharide, which is biocompatible and gelled at room temperature. Agarose gel has been investigated for neural and cartilage tissue-engineering delivery vector (Tripathi, Kathuria, & Kumar, 2009). Agarose is also taken as an optimal material to use in a nerve regeneration scaffold based on its biocompatibility, inertness, and stability in the spinal cord (Gros, Sakamoto, Blesch, Havton, & Tuszynski, 2010; Stokols & Tuszynski, 2004). However, the major drawback of agarose gel is low cell adhesiveness and slow degradation rate. For extending its applications in tissue regeneration, it is necessary for agarose to be composited with other fast degradable biomaterial, for example HA.

The aim of this work was to prepare a controlled degradation composite agarose/HA hydrogel, and to disclose the effect of agarose/HA ratio on morphology, equilibrium swelling, thermal stability and in vivo degradation of the composite agarose/HA hydrogel for evaluating its potential application in biomedical engineering, such as drug delivery, tissue engineering and wound healing.

* Corresponding author. Tel.: +86 020 85220469; fax: +86 020 85220469.
E-mail address: tshunqt@jnu.edu.cn (S.-Q. Tang).

0144-8617/$ – see front matter © 2012 Elsevier Ltd. All rights reserved.
doi:10.1016/j.carbpol.2012.02.050

2. Materials and methods

2.1. Materials and animals

Agarose was supplied by MDBio, Inc. (Spain). Sodium salt of hyaluronic acid was purchased from Freda biopharm Co. Ltd. (China). All other commercial reagents were of analytical grade and were used without further purification. The specific pathogen free (SPF) Kunming mice of 6–8 wk old, female, weighing from 23 to 27 g, were purchased from the Experimental Animal Center of Guangdong Province, China.

2.2. Preparation of composite agarose/HA hydrogel

Composite agarose/HA hydrogel was prepared according to previously described (Chang, Duan, & Zhang, 2009) with some modifications. Briefly, agarose was dispersed into 6 wt% NaOH solution with stirring for 4 h, and then rinsed repeatedly until the pH of supernatant was neutral. The alkali treated agarose was collected and freeze-dried to obtain agarose powder. 3 g agarose powder was dissolved in boiling deionized water with a concentration of 3 wt%, and cooled to 40 °C. HA was dissolved in 40 °C deionized water to make a 3 wt% solution. Agarose solution was rapidly mixed with HA one with different weight ratios of agarose and HA by 10:1, 8:3, and 5:5. The resultant solution was stirred at 40 °C for 1 h to get a homogeneous solution respectively. After this, a mixture of epichlorohydrin (1 mL) and 20% alkaline solution (1 mL) was added to 10 mL of the above composite agarose/HA solution. And then the system reacted at 60 °C to form hydrogel, named as composite agarose/HA hydrogel 1–3 (abbreviated as C1, C2 and C3). Finally, composite agarose/HA hydrogel was taken out carefully and immersed in distilled water to remove the residual ECH or others for 1wk. During this process, distilled water was replaced three times for 1d.

2.3. SEM

Morphologies of agarose, mixture of agarose/HA (weight ratio being 5:5) without crosslinking and C1, C2 and C3 were observed under SEM after these samples were freeze-dried and then gold-coated using a Cressington 108 Auto (Cressington, Watford UK). The surface and cross-sectional morphologies were observed under a JSM-6330F SEM (JEOL, Peabody, MA) operated at 20 kV accelerating voltage.

In order to disclose the micro-structural changes of these hydrogels, AFM was also applied to test the samples (see Supplementary data).

2.4. FT-IR spectra

FTIR spectra of agarose, HA and the freeze-dried C1, C2 and C3 were recorded with FTIR spectrometer (Nicolet Avatar 360, USA) against a blank KBr pellet background.

2.5. Thermo-gravimetric analysis

Thermal gravimetric analysis (TGA) of the freeze-dried C1, C2 and C3 was carried out by using thermogravimetric analysis equipment (SDT Q600, TA, USA). Samples were placed in the sealed aluminum cells and heated from 30 to 600 °C at a heating rate of 10 °C min^{-1} in nitrogen atmosphere.

2.6. WAXD analysis

X-ray diffraction patterns of the freeze-dried C1, C2 and C3 were recorded by an X-ray diffraction diffractometer (MSAL-XRD2, Bragg Science and Technology Co., Ltd., Beijing) with Cu Kα radiation (λ = 1.5406 Å) over the interval 5–40°/2θ. Radiation from the anode operated at 36 kV and 20 mA, monochromized with a scanning speed 4°/min. Individual crystal reflection peaks and the amorphous background were extracted by the curve-fitting process of the integrated diffraction intensity profile. Background intensity was subtracted before peak fitting. Each intensity spectrum was fitted by employing a Gaussian function as the peak profile.

2.7. Swelling measurement

The swelling ratio of the freeze-dried hydrogel was measured with gravimetric method in PBS (pH 7.4) at 37 °C for 24 h. The swollen hydrogel was removed and immediately weighed with a microbalance after the surface excess of water was absorbed with filter paper. The equilibrium swelling ratio (ESR) of hydrogel was calculated as following (n = 3),

$$\mathrm{ESR} = \frac{W_s - W_d}{W_d}$$

where W_s is the weight of the swollen hydrogel at 37 °C, and W_d is the weight of the freeze-dried hydrogel.

2.8. In vitro cytotoxicity assay

The cytotoxicity of the hydrogel was assessed by MTT assay. The extracted medium of hydrogel was prepared by incubating the freeze-dried hydrogel with 10% fetal bovine serum (FBS) for 24 h. Then the extract was diluted with culture medium into different concentrations for the direct cell counting test. 3T3 fibroblasts were seeded in 96-well plate at a density of 10^4 cells per well supplementing 100 μL of DMEM containing 10% FBS. After 24 h incubation, 100 μL of extracted media of different hydrogels in given concentrations were added, respectively. After additional incubation for 72 h, these cells cultured in per well received 25 μL of MTT (5 mg/mL), followed by incubation at 37 °C for 4 h, then the medium was replaced by 200 μL of dimethylsulfoxide (DMSO), and the absorbance of DMSO was measured at 570 nm. The cell viability was calculated as a percentage ratio of the absorbance of the experiment group and PBS group as control one.

2.9. Implantation assay

The implantations were performed in accordance with the Guidelines of the Care and Use of Laboratory Animals published by the China National Institute of Health. The mice were anesthetized by intraperitoneal injection of sodium pentobarbital. After shaving and disinfection, subcutaneous pockets were made to the right and the left of one midline incision on the back.

Both sides were implanted with the same freeze-dried hydrogel (n = 3), and the wounds were sutured. At intervals of 1, 2, 3, 4, 5, 6, 8, 10 and 13 wk postoperation, mice were sacrificed. The implantations with surrounding tissue and underlying muscle were carefully dissected from the subcutaneous site and fixed with 2.5% (v/v) glutaraldehyde in 0.1 M PBS buffer at 4 °C for at least 24 h.

The degradation of the composite agarose/HA hydrogel was quantitatively analyzed by weighing the residues in different time. Prior to weigh, the tissue capsules were cleared away carefully, rinsed and freeze-dried. The weight loss of C1, C2 or C3 was calculated as following (n = 3),

$$\mathrm{DR}\ (\%) = \left(\frac{W_0 - W_t}{W_0}\right) \times 100$$

where DR means degradation rate, W_0 is the pre-implantation weight of the freeze-dried hydrogel, and W_t is the post-implantation weight of the freeze-dried hydrogel.

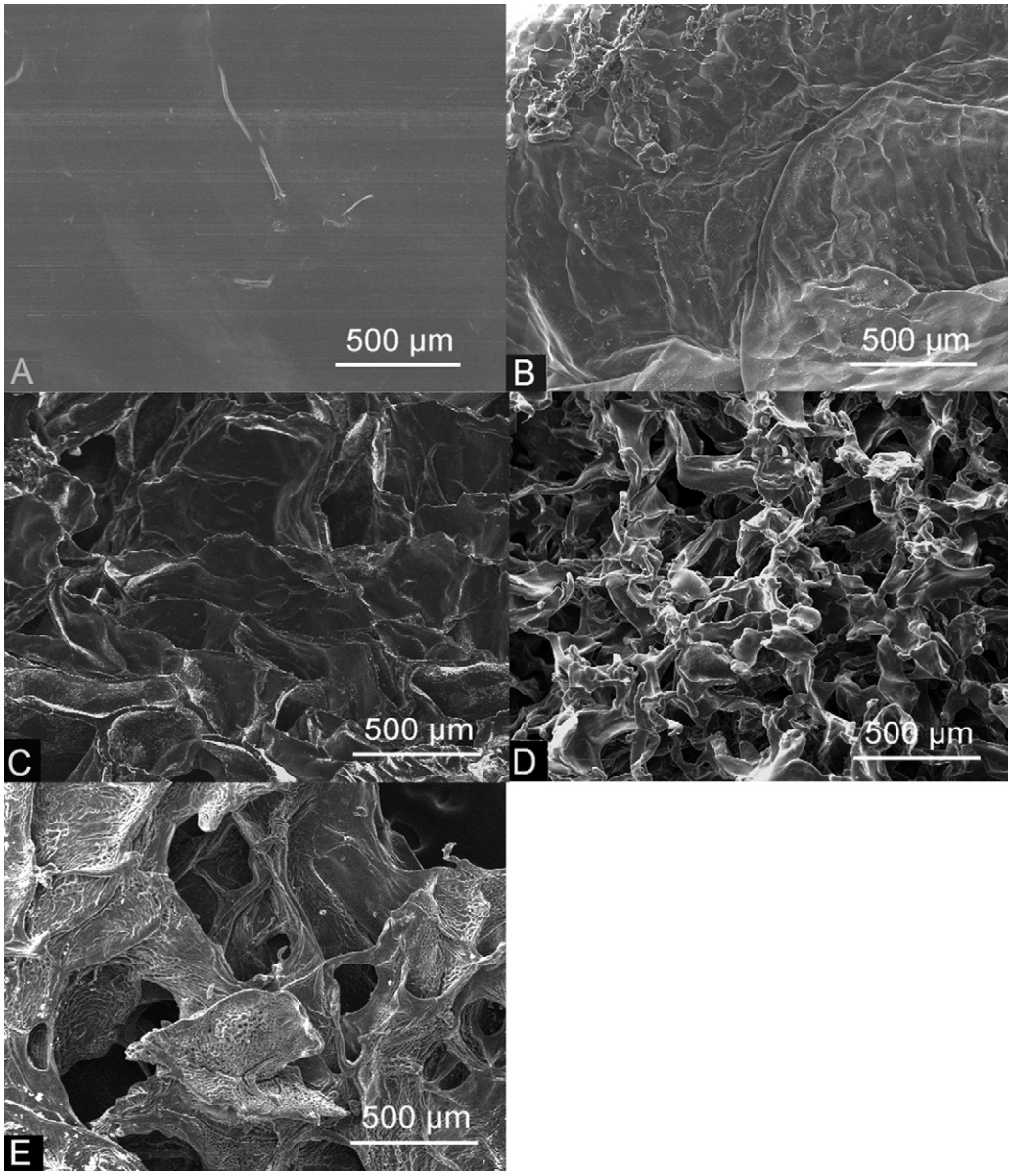

Fig. 1. SEM images of the sponge surface of agarose (A), mixture of agarose/HA (B), C1 (C), C2 (D) and C3 (E).

For histological analyses, the harvested samples were embedded into paraffin, sectioned with a thickness of 3 μm, and then stained by hematoxyline–eosin (H&E), and visualized by an optical microscope (Nikon TE-2000 inversion microscope, Japan).

2.10. Statistical analysis

The experimental data were analyzed using Analysis of Variance (ANOVA). Statistical significance was set to $p < 0.05$. Results are presented as mean ± standard deviation.

3. Results and discussion

3.1. Material properties

From SEM morphologies, it can be seen (Fig. 1A) that agarose sponge had a smooth surface, but the mixture of agarose/HA (5:5) without crosslinking had a rough one with few pores (Fig. 1B). However, the freeze-dried C1, C2 or C3 displayed a loose and porous structure, and C2 showed more homogenous structure. The average pore diameter of C1 to C3 increased with HA content, from the range of 150–500 μm to 300–1000 μm (Fig. 1C–E). This means that HA content has significant effect on the morphologies of the composite agarose/HA hydrogels. When agarose was major in the composite agarose/HA hydrogel, the increase of HA contributed to form homogeneous and interconnectively porous structure in the composite agarose/HA hydrogel. Nevertheless, the higher HA content (over 50%) in the composite agarose/HA hydrogel results in the formation of heterogenous pores and tighter network structure (Tan, Ramirez, et al., 2009).

From AFM images (Suppl. Fig. 1), remarkable differences can be observed between the single agarose or HA membrane and the composite agarose/HA films. After crosslinking, the composite agarose/HA films became rougher in contrast with agarose or HA membrane. The rough surface can be assigned to HA embedding into molecular chain of agarose, which destroys the uniform structure of agarose and changes the roughness of agarose in microdomain.

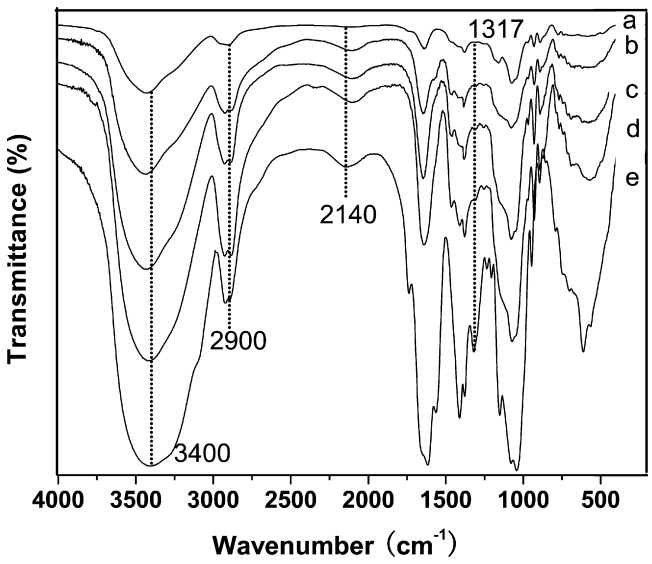

Fig. 2. FTIR spectra of agarose (a), C1 (b), C2 (c), C3 (d), and HA (e).

3.2. FT-IR

As can be seen from FTIR spectra (Fig. 2), the peak assigned to O—H bond stretching vibration at 3200–3700 cm^{-1} (Wu & Liao, 2005) was much more intense for composite agarose/HA hydrogel comparing with that for agarose, which is due to much more —OH groups of hyaluronic acid in the composite agarose/HA hydrogel. Moreover, with the increase of HA in the composite agarose/HA hydrogel, the stretching vibration of amide in HA also contributes to the intensity of the vibration absorption peak around 3400 cm^{-1}. Compared with agarose, the peaks around 2900 cm^{-1} and 1317 cm^{-1} in the spectra of HA and composite agarose/HA hydrogel became more intense, which was assigned to the stretching vibration of methyl, while near 2140 cm^{-1} to the imines in HA.

3.3. TGA

The changes of structures or compositions in polysaccharides are usually reflected in their TGA thermograms. The early minor weight loss of agarose (Fig. 3(A)) or HA (Fig. 3(B)) is attributed to desorption of water bonded by hydrogen bonds between about 30 and 115 °C. The subsequent major weight loss of agarose or HA appeared at temperature of 270–330 °C or 210–244 °C, respectively. This is attributed to the decompositions of these two polysaccharides.

There are great differences between single agarose or HA hydrogel and composite agarose/HA hydrogel in their TGA thermograms. From Fig. 3(D)–(F), the freeze-dried C1 ~ C3 showed similar initial weight loss at about 140 °C due to the removal of water. In comparison with agarose or HA hydrogel, the temperature of water desorption increased about 20 °C. It may be attributed to tighter linking through polar interactions with carboxylate groups in the composite agarose/HA hydrogel (Laurienzo, Malinconico, Motta, & Vicinanza, 2005). The second stage from about 140 to 340 °C and the third stage from 340 to 500 °C in the TG graph may due to the decomposition of different chemical structures of the composite agarose/HA hydrogel. Besides, there is a close relationship between component and degradation temperature of the composite hydrogel, which can be deduced from the initial temperature of the third stage evidently. When the ratio of HA and agarose increased from 1:10 to 3:8, the initial temperature of the third stage risen from 335 °C to 347 °C due to the increase of crosslinking degree. However, the thermal stability of composite agarose/HA hydrogel decreased when HA content increased (Fig. 3(F)).

Comparing to the TG thermograms of agarose/HA with or without crosslinking with the same component ratio (5:5), thermal characteristics of agarose/HA hydrogel without crosslinking (Fig. 3(C)) depended on HA, which can be reflected from in the temperature range of 30–100 °C and 211–257 °C corresponding to the dehydration temperature and the decomposition temperature. This means that the thermal stability will not be strengthened through mixing without crosslinking, and the intermolecular interactions are weak between agarose and HA. However, the dehydration temperature extended from 100 °C to about 140 °C and one sharp drop

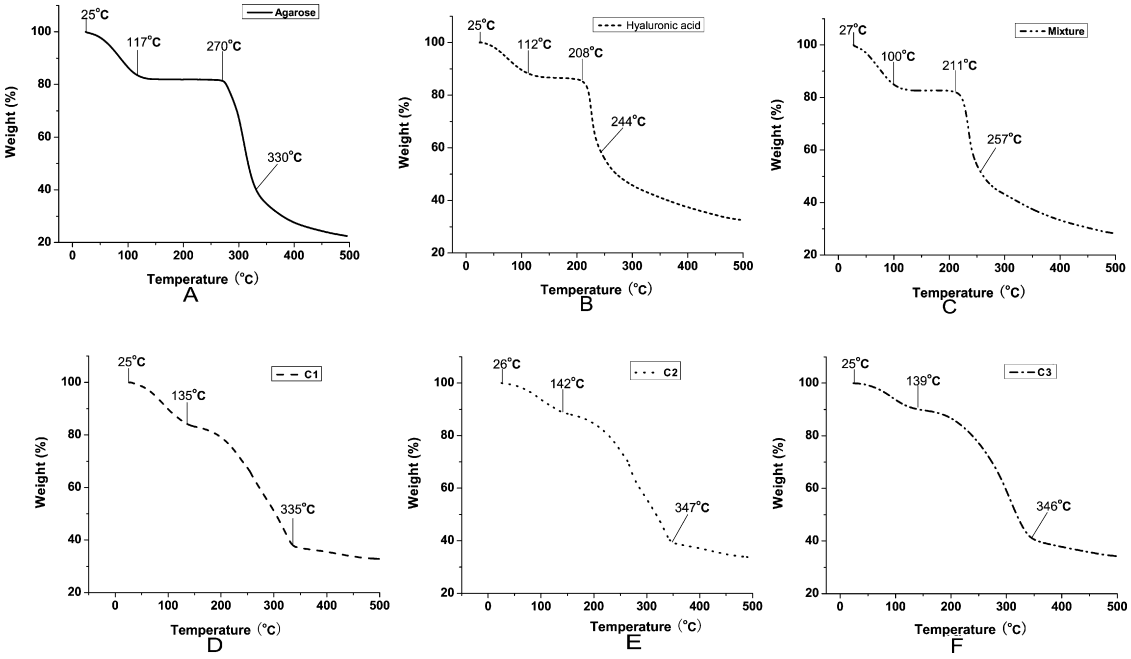

Fig. 3. TGA thermograms for agarose (A), HA (B), mixture of agarose/HA (C), C1 (D), C2 (E) and C3 (F).

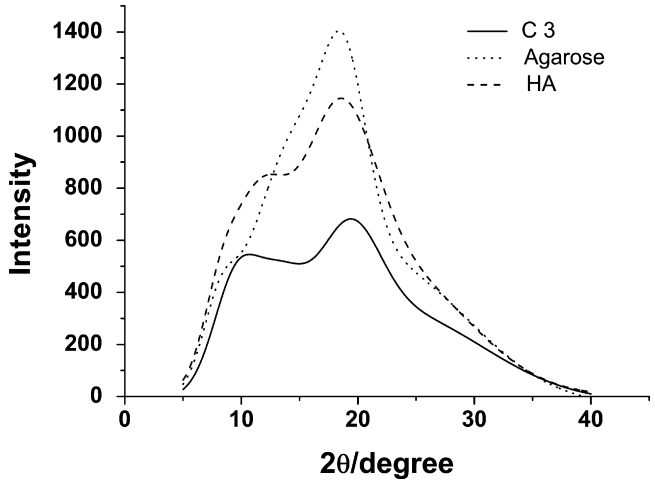

Fig. 4. WXRD patterns of agarose, HA and C3.

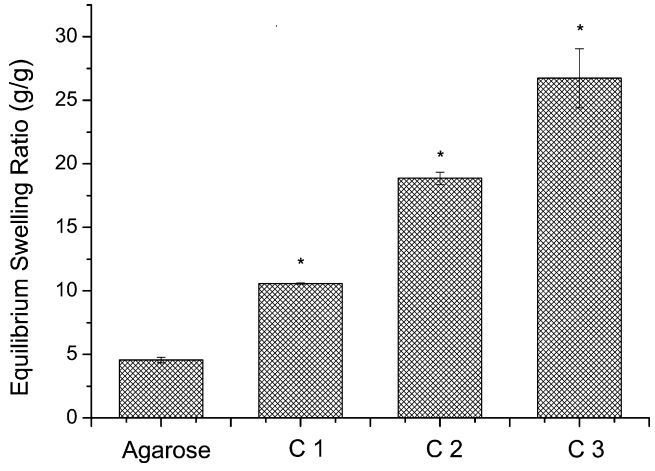

Fig. 5. Equilibrium swelling ratio of agarose and composite hydrogels as a function of weight ratio incubated in PBS at 37 °C. (Values reported are an average of $n = 3$; *denotes statistically significant difference, $p < 0.05$.)

was found in the range from about 140 to 346 °C (Fig. 3(F)). This indicated that relatively high thermal stability appeared in C3, suggesting that there is the chemical crosslinking between agarose and HA in the hydrogel.

3.4. WXRD

Further evidences for the formation of composite agarose/HA hydrogel were obtained from XRD graphs. Fig. 4 shows WXRD patterns of agarose, HA, and the freeze-dried C3. The diffraction peaks at $2\theta = 20°$ corresponded to the (1 1 0) plane of agarose crystalline form. Those at 12° and 20° were assigned to HA. If an intrinsic inclusion complex is formed, the diffraction pattern of the complex would be clearly distinct from the superposition of every component in the complex (Zeng, Ren, Zhou, Yu, & Chen, 2011). It showed that C3 exhibited greater amorphous morphology than agarose or HA. The characteristic peaks of agarose or HA significantly lowered or disappeared in C3. The result proved again that chemical crosslinking occurred between agarose and HA, which destroyed the initial crystalline structure of agarose and HA.

3.5. Equilibrium swelling ratio

Fig. 5 indicates the equilibrium swelling ratios of the freeze-dried C1–C3 in PBS. The swelling ratio increased along with increase

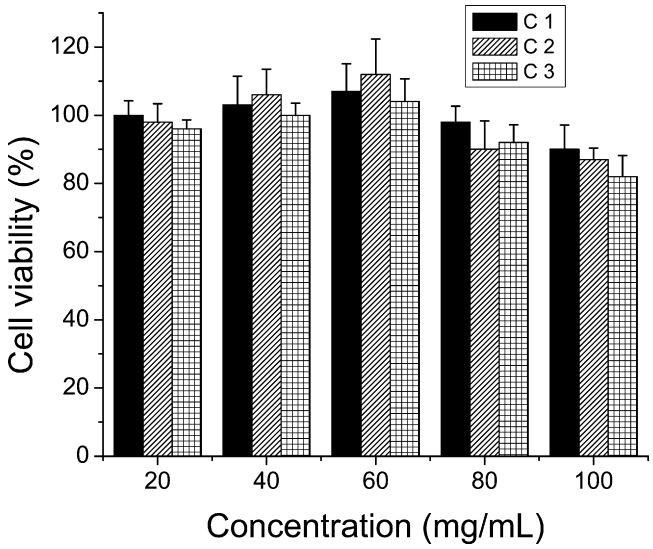

Fig. 6. Cytotoxicity of agarose/HA complex at various concentrations against 3T3 fibroblast ($n = 5$, Mean ± SD). Cells were seeded at a density of 10^4 cells/well in 96-well plates. Cell viability of cells treated with different concentration polymers was measured after 72 h by MTT assay.

of HA content for its remarkable absorbing abilities to fluids and high water retention capacity (Mao, Liu, Yin, & Yao, 2003; Park, Lee, Lee, & Suh, 2003; Volpi, Schiller, Stern, & Soltes, 2009). In Fig. 5, agarose can absorb water about 4.6 folds to its dry weight, while the swelling ratios of C1–C3 reach 10.6, 18.9 and 26.7 folds respectively. Swelling properties of the as-prepared hydrogels are crucial for substance exchange when they are used as scaffolds in biomedical applications. The enhanced water swelling capacity may owe to the interconnective porous, which led to capillarity and accumulation of water. Besides, the hydrophilic groups, such as hydroxyl and carboxyl groups, can easily produce hydration with water (Tan, Chu, Payne, & Marra, 2009).

3.6. In vitro cytotoxicity

Under optical microscope (Suppl. Fig. 2), the cell morphologies of 3T3 fibroblasts cultured with the extract medium in a concentration of 10 mg/mL was normal. The histogram showed that no significant cytotoxicity was found even the concentration of the extract medium in culture medium reached 40 mg/mL. Moreover, the extract medium promoted the proliferation of 3T3 fibroblasts within the concentration of 10 mg/mL (Fig. 6). This may be attributed to the biological function of HA dropping from the hydrogel during extraction to promote the growth of fibroblasts (David-Raoudi et al., 2008; Yoneda, Yamagata, Suzuki, & Kimata, 1988). The result is consistent with previous report on 3T3 fibroblasts, which was assigned to a stimulatory effect of HA on cell proliferation (Moon, Lee, & Kim, 1998).

3.7. Hydrogel degradation in vivo

The implantation suffered from a series of physiochemical processes. In Suppl. Table 1, the weight loss percentages of agarose group were 3.50 ± 1.80%, 6.65 ± 2.52%, 15.00 ± 3.00% and 23.65 ± 3.33%, which were corresponding to the post-implantation for 1, 2, 3 and 4 wk respectively. However, the weight loss percentages of C3 were 10.50 ± 4.77%, 31.84 ± 4.25%, 66.15 ± 5.00% and 100%, respectively. This result showed that the degradation rate of C3 was much faster than agarose sponge. The incorporation of HA into the hydrogel increased biological activity and improved the degradation of C3. As a candidate for regenerative scaffold, it is

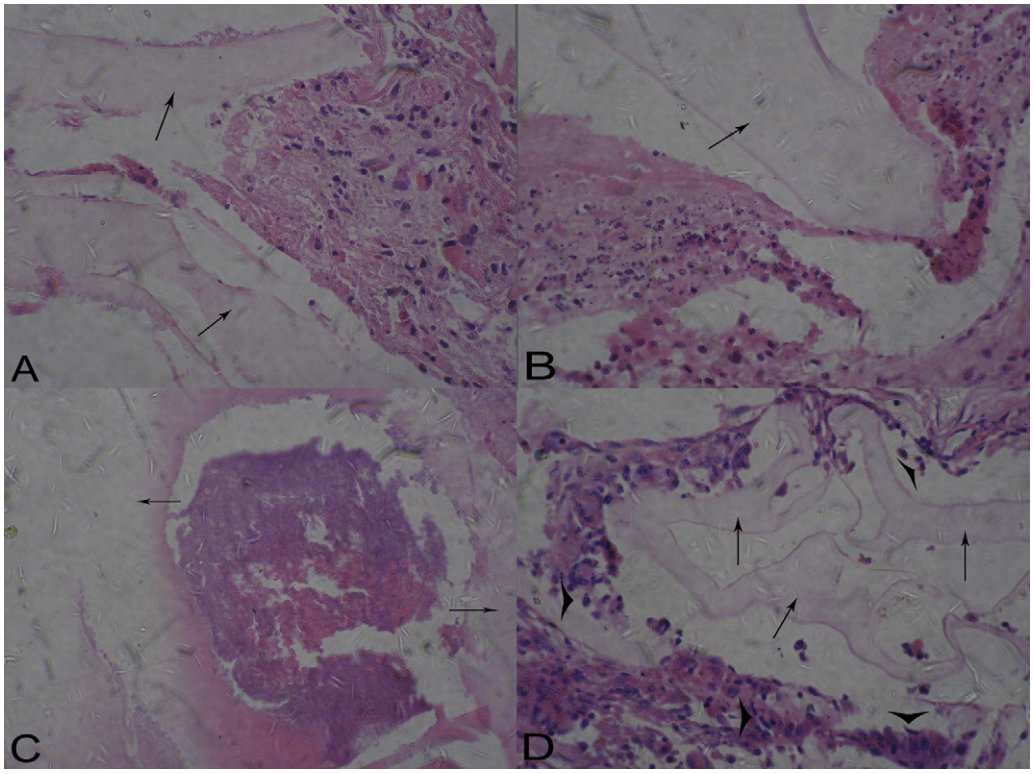

Fig. 7. Time course after implantation of agarose sponge (HE staining) (original magnification 400×): (A) after 1 wk; (B) after a month; (C) after 2 mo.; (D) after 3 mo. Arrows show fragments of the implant and head arrows show inflammatory cells.

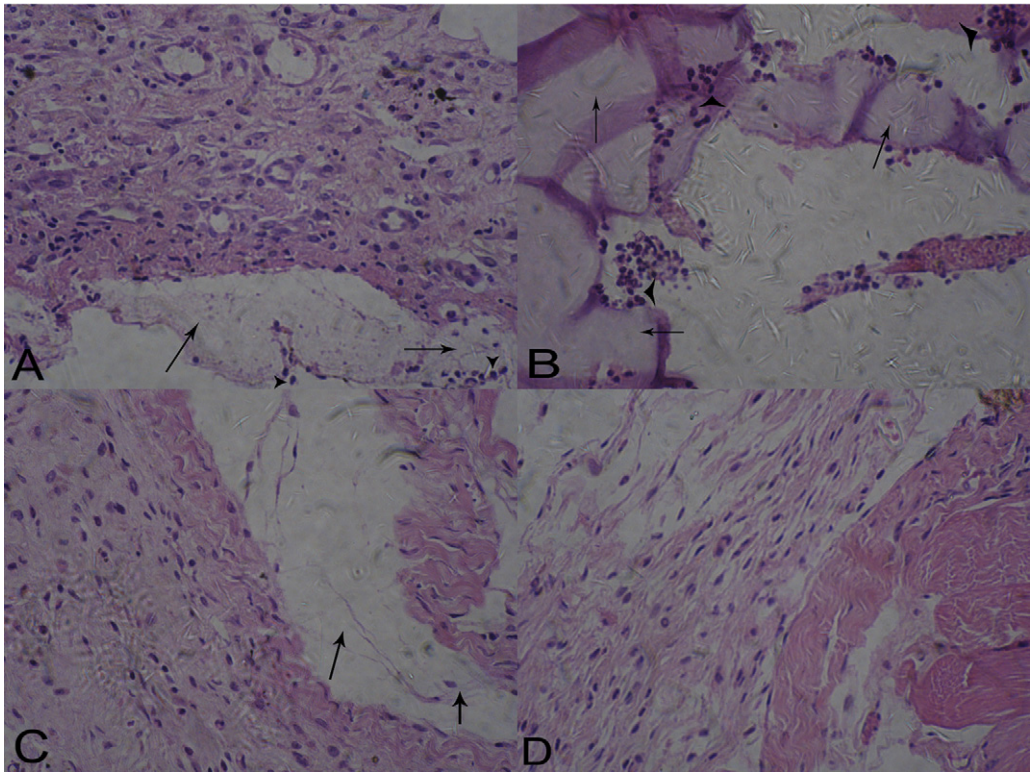

Fig. 8. Time course after implantation of C1 (HE staining) (original magnification 400×): (A) after 1 wk; (B) after 3 wk; (C) after 6 wk; (D) after 8 wk. Arrows show fragments of the implant and head arrows show inflammatory cells.

important for the composite agarose/HA hydrogel to be degradable. In this study, as we have known that agarose is hardly degradable in vivo, the degradable agarose/HA hydrogel is favorable to extend the applications of agarose in tissue engineering or regenerative medicine.

3.8. Histological observation

Results of histological examination (Fig. 7) showed that after 3 mo. implantation, agarose did not show apparent degradation because it is no agarose enzyme in mouse body (Moon et al., 1998). There is a slight inflammation in agarose implantation within a short term (Fig. 7(A and B)). A slight circumferential fibrous capsule around agarose was observed dotting a lot of macrophages and fibroblasts, which was accompanied by a minimal inflammation of polymorphonuclear cells after 1 wk. However, agarose as a foreign existing in organism for a long term aggregated inflammatory reactions (Fig. 7(C and D)). This reflects the disadvantages of inert materials even with good biocompatibility, for the host response including inflammation happened through the whole implantation.

We can see the degradation process of C1, C2 and C3 in Fig. 8, Suppl. Fig. 3 and Suppl. Fig. 4, which showed that C1 ~ C3 almost disappeared within 8, 5 and 4 wk post-implanatation, respectively. In the initial stage, the inflammatory cells migrate to the surrounding of implants, and a slight capsule of fibroblasts and macrophages was formed with inflammatory responses. Then the inflammatory cells climbed into the implants and broke implants in pieces gradually swallowed the pieces. There is a close relationship between inflammation and content of HA in these hydrogels. Generally, the inflammatory response appeared a little quicker in composite agarose/HA hydrogel than in agarose in short term, and the inflammation reactions were a little more serious with increase of HA. Previous studies showed that HA act as a promoter of early inflammation, through stimulating the migration of inflammatory cells (Picart et al., 2005), as well as enhancing cellular infiltration and production of proinflammatory cytokines (Kobayashi & Terao, 1997; Wisniewski et al., 1996). In the current opinion, the first inflammation phase is considered as the preparation for the tissue formation and the tissue remodeling phase. The inflammation response on an appropriate level would provide benefits for the healing progression. In the process of inflammation, the cellular ingrowth was accompanied by the degradation of the implant. The degradation also varied with the ratio of agarose and HA in hydrogel. Our studies found that the increase of HA accelerated the degradation of the composite agarose/HA hydrogel. It indicates that HA plays an important role in the degradation of composite hydrogels. Generally, HA is rapidly exhausted in the body by hyaluronidase, with half-life ranging from hours to days in tissue (Burdick & Prestwich, 2011). However, there is no specific enzyme for agarose in vivo, which makes agarose hardly to be degraded. In present study, composite agarose/HA hydrogels can be degraded within certain degradation time. This can be explained from the changes of morphology and structure of composite agarose/HA hydrogel, vacancies formation after quick degradation of HA, as well as the phagocytosis of immune cells. On one hand, HA was composited into agarose to break the filament structure of agarose sponge and form the interconnective pores in the composite hydrogel, which increased the degradation site of hydrogel in medium. On the other hand, multiple vacancies formed in the hydrogel and the hydrogel was destroyed into debris after quick degradation of HA, and finally the agarose debris in implantations were cleared away gradually by phagocytosis of immune cells which are called by HA at initial stage of implantation.

4. Conclusions

The crosslinking composite agarose/HA hydrogels were synthesized successfully, and achieved modification of agarose with the physicochemical properties and biological properties. The addition of HA into agarose hydrogel significantly increased pore size, swelling ratio and thermal stability. The crosslinking composite agarose/HA hydrogels presented little cytotoxicity in vitro, and their in vivo inflammatory response was mild. The composite hydrogels with higher HA content showed faster degradation rate than that with lower HA. The degradation time can be controlled by altering the ratio of agarose and HA. These characteristics demonstrate that crosslinking composite agarose/HA hydrogel has great potential application in arthritis treatment, wound healing, drug delivery, and tissue engineering.

Acknowledgements

This project is supported by the 863 high-tech plan (2007AA09Z436), NNSFC (31070853), and Guangdong Tech Plan (2010B031100015) and Guangzhou Tech Plan (2010EJ-0041), and the Fundamental Research Funds for the Central Universities (China). The authors also thank Dr Xiang Min, Hao Ma and Ling-Hui Zhang for providing helps in experiments and data analysis.

Appendix A. Supplementary data

Supplementary data associated with this article can be found, in the online version, at doi:10.1016/j.carbpol.2012.02.050.

References

Burdick, J. A., & Prestwich, G. D. (2011). Hyaluronic acid hydrogels for biomedical applications. *Advanced Materials*, *23*, H41–H56.
Chang, C. Y., Duan, B., & Zhang, L. N. (2009). Fabrication and characterization of novel macroporous cellulose–alginate hydrogels. *Polymer*, *50*, 5467–5473.
Choh, S. Y., Cross, D., & Wang, C. (2011). Facile synthesis and characterization of disulfide-cross-linked hyaluronic acid hydrogels for protein delivery and cell encapsulation. *Biomacromolecules*, *12*, 1126–1136.
David-Raoudi, M., Tranchepain, F., Deschrevel, B., Vincent, J. C., Bogdanowicz, P., Boumediene, K., et al. (2008). Differential effects of hyaluronan and its fragments on fibroblasts: Relation to wound healing. *Wound Repair and Regeneration*, *16*, 274–287.
Deshmukh, M., Singh, Y., Gunaseelan, S., Gao, D. Y., Stein, S., & Sinko, P. J. (2010). Biodegradable poly(ethylene glycol) hydrogels based on a self-elimination degradation mechanism. *Biomaterials*, *31*, 6675–6684.
Gros, T., Sakamoto, J. S., Blesch, A., Havton, L. A., & Tuszynski, M. H. (2010). Regeneration of long-tract axons through sites of spinal cord injury using templated agarose scaffolds. *Biomaterials*, *31*, 6719–6729.
Hawkins, A. M., Milbrandt, T. A., Puleo, D. A., & Hilt, J. Z. (2011). Synthesis and analysis of degradation, mechanical and toxicity properties of poly(beta-amino ester) degradable hydrogels. *Acta Biomaterialia*, *7*, 1956–1964.
Kobayashi, H., & Terao, T. (1997). Hyaluronic acid-specific regulation of cytokines by human uterine fibroblasts. *The American Journal of Physiology*, *273*, C1151–C1159.
Laurienzo, P., Malinconico, M., Motta, A., & Vicinanza, A. (2005). Synthesis and characterization of a novel alginate-poly (ethylene glycol) graft copolymer. *Carbohydrate Polymers*, *62*, 274–282.
Mao, J. S., Liu, H. F., Yin, Y. J., & Yao, K. D. (2003). The properties of chitosan–gelatin membranes and scaffolds modified with hyaluronic acid by different methods. *Biomaterials*, *24*, 1621–1629.
Moon, S. O., Lee, J. H., & Kim, T. J. (1998). Changes in the expression of c-myc, RB and tyrosine-phosphorylated proteins during proliferation of NIH 3T3 cells induced by hyaluronic acid. *Experimental and Molecular Medicine*, *30*, 29–33.
Park, S. N., Lee, H. J., Lee, K. H., & Suh, H. (2003). Biological characterization of EDC-crosslinked collagen–hyaluronic acid matrix in dermal tissue restoration. *Biomaterials*, *24*, 1631–1641.
Picart, C., Schneider, A., Etienne, O., Mutterer, J., Schaaf, P., Egles, C., et al. (2005). Controlled degradability of polysaccharide multilayer films in vitro and in vivo. *Advanced Functional Materials*, *15*, 1771–1780.
Segura, T., Anderson, B. C., Chung, P. H., Webber, R. E., Shull, K. R., & Shea, L. D. (2005). Crosslinked hyaluronic acid hydrogels: A strategy to functionalize and pattern. *Biomaterials*, *26*, 359–371.
Stokols, S., & Tuszynski, M. H. (2004). The fabrication and characterization of linearly oriented nerve guidance scaffolds for spinal cord injury. *Biomaterials*, *25*, 5839–5846.

Tan, H. P., Chu, C. R., Payne, K. A., & Marra, K. G. (2009). Injectable in situ forming biodegradable chitosan–hyaluronic acid based hydrogels for cartilage tissue engineering. *Biomaterials*, *30*, 2499–2506.

Tan, H. P., Ramirez, C. M., Miljkovic, N., Li, H., Rubin, J. P., & Marra, K. G. (2009). Thermosensitive injectable hyaluronic acid hydrogel for adipose tissue engineering. *Biomaterials*, *30*, 6844–6853.

Toole, B. P. (2004). Hyaluronan: From extracellular glue to pericellular cue. *Nature Reviews Cancer*, *4*, 528–539.

Tripathi, A., Kathuria, N., & Kumar, A. (2009). Elastic and macroporous agarose–gelatin cryogels with isotropic and anisotropic porosity for tissue engineering. *Journal of Biomedical Materials Research Part A*, *90A*, 680–694.

Volpi, N., Schiller, J., Stern, R., & Soltes, L. (2009). Role, metabolism, chemical modifications and applications of hyaluronan. *Current Medicinal Chemistry*, *16*, 1718–1745.

Wisniewski, H. G., Hua, J. C., Poppers, D. M., Naime, D., Vilcek, J., & Cronstein, B. N. (1996). TNF/IL-1-inducible protein TSG-6 potentiates plasmin inhibition by inter-alpha-inhibitor and exerts a strong anti-inflammatory effect in vivo. *Journal of Immunology*, *156*, 1609–1615 (Baltimore, Md: 1950)

Wu, C. S., & Liao, H. T. (2005). A new biodegradable blends prepared from polylactide and hyaluronic acid. *Polymer*, *46*, 10017–10026.

Yoneda, M., Yamagata, M., Suzuki, S., & Kimata, K. (1988). Hyaluronic-acid modulates proliferation of mouse dermal fibroblasts in culture. *Journal of Cell Science*, *90*, 265–273.

Zeng, J., Ren, Y., Zhou, C., Yu, S., & Chen, W. H. (2011). Preparation and physicochemical characteristics of the complex of edaravone with hydroxypropyl-β-cyclodextrin. *Carbohydrate Polymers*, *83*, 1101–1105.